Viser Technology Pte. Ltd.
Research and Application of Materials Science
DOI: 10.33142/rams.v4i2.8466

Research Article Open Access

Effect of electric pulse rolling on plastic forming ability of AZ91D magnesium alloy

Xinyu LIU[1], Yuezhang ZHOU [1], Wenjie BO [1], Yong ZHANG [2], Guihong GENG [1*]

1 School of Materials Science and Engineering, North Minzu University, Yinchuan 750021, P.R. China
2 State Key Laboratory for Advanced Metals and Materials, University of Science and Technology Beijing, Beijing 100083, China.

***Corresponding Author:** Guihong GENG, E-mail: gengguihong@nmu.edu.cn*

Abstract:
AZ91D magnesium alloy rolled under four rolling conditions, namely cold rolling, electric pulse cold rolling, hot rolling and electric pulse hot rolling, and the first principles calculation of Mg with or without external electric field carried out. The results show that: The application of pulse current in the rolling process of AZ91D magnesium alloy can effectively improve the edge crack of the sample, optimize the texture of AZ91D magnesium alloy and reduce its texture strength, promote the generation of tensile twins and the transition from small Angle grain boundaries to large Angle grain boundaries, and thus improve the plastic forming ability of AZ91D magnesium alloy. Make it more prone to plastic deformation. Compared with ordinary rolling, the microhardness of α-Mg matrix decreases by 15%. The tensile strength and elongation increased from 137MPa and 3.4% to 169MPa and 4.7%, respectively. The results show that the stiffness of Mg decreases and the Poisson's ratio of Mg increases when the electric field applies. When the B/G value is greater than 1.75, the plasticity of Mg is improved. The fault energy at the base surface of Mg does not change much, while the fault energy at the prismatic surface of Mg decreases obviously, showing the external electric field mainly affects the prismatic surface slip of Mg, which makes the prismatic surface slip easier to start, and thus improves the plastic forming ability of Mg.
***Keywords:** Electric pulse rolling; Electroplasticity; AZ91D; First principles calculation*

1 Introduction

Magnesium alloy has become one of the lightweight process materials in the new century due to its high specific strength and stiffness, low density, good electrical and thermal conductivity, and good damping and shock absorption [1-2]. Its structural parts have wide application prospects in automotive, aerospace, and communication fields [3-5]. However, magnesium metal belongs to the dense row hexagonal crystal structure, only the base plane ＜a＞ can open the slip at room temperature [6], so its room temperature deformation ability is poor, it is difficult to carry out mass industrial production by cold deformation, which greatly limits the application of magnesium alloy in industry, so magnesium alloy mostly adopts the method of hot forming [7]. However, under hot forming conditions, there are problems such as reduced die life, roughness of magnesium alloy surface, increased thermal stress of magnesium alloy and higher energy consumption [8].

In recent years, it has shown the application of certain pulsed currents during the deformation of metallic materials can effectively improve their plastic forming ability, a phenomenon known as the electroplastic effect. Indhiarto et al [9] performed unidirectional tensile experiments on AZ31B magnesium alloy by applying pulsed currents with different peak current densities at the same temperature. The results showed the ultimate tensile strength gradually decreases with increasing peak current density, independent of temperature. This proves that the non-thermal effect of pulsed current has a positive effect on the tensile properties. Liu et al [10] conducted tensile tests on AZ31B magnesium alloy sheet with different frequencies of pulsed current and showed the pulsed current did not change the initial yield stress of the magnesium alloy, but reduced the work-hardening rate and produced a softening effect. In addition, the electroplastic effect was controlled by thermal activation. Although the electroplastic effect of magnesium alloys has been studied by a large number of researchers, the mechanism of the action of current on magnesium alloys is still unclear. In 1968 Vitek [11] proposed the concept of generalized layer fault energy and applied it to the calculation of plastic forming ability of magnesium alloys. Yuasa et al [12] calculated the generalized layer fault energy of Mg, Mg-Zn-Ga, Mg-Ga and Mg-Zn. The calculation results showed that the addition of Ca and Zn reduced the plastic anisotropy of magnesium alloys, which was due to the unstable base slip in the alloy due to the nonlinear nature of the layer error energy.

Received on November 4, 2022; Accepted on December 13, 2022

In this paper, AZ91D magnesium alloy rolled under four rolling conditions: ordinary cold rolling (CR), electric pulse cold rolling (EPC-CR), ordinary hot rolling (HR) and electric pulse hot rolling (EPC-HR). EBSD analysis and theoretical calculation performed on AZ91D magnesium alloy after electric pulse rolling to investigate the effect of electric pulse rolling on the plastic forming ability of AZ91D magnesium alloy.

2 Experimental materials and methods

2.1 Experimental materials

Commercial AZ91D magnesium alloy sheet is selected as the experimental material, and its main components are shown in Table 1. The AZ91D magnesium alloy sheet was cut into 60×12×3mm experimental sheet by wire-cutting equipment. The experimental sheet was held at 400℃ for 3h before use, and then completely annealed by air cooling.

Table 1 Main components of AZ91D magnesium alloy

Element	Al	Zn	Mn	Si	Cu	Mg
wt.%	9	0.67	0.25	0.05	0.015	Others

2.2 Electric pulse rolling process of AZ91D magnesium alloy

AZ91D magnesium alloy rolling experiment adopts strong pulse current rolling equipment independently developed by the research group, which is mainly composed of four-roll rolling equipment and strong pulse power supply. Pressure sensors are equipped on the rolls to display the pressure between the upper and lower rolls in real time. The strong pulse rolling equipment and its working principle are shown in Figure 1. The peak current and current frequency in the rolling process can be displayed by the equipment sensor and oscilloscope.

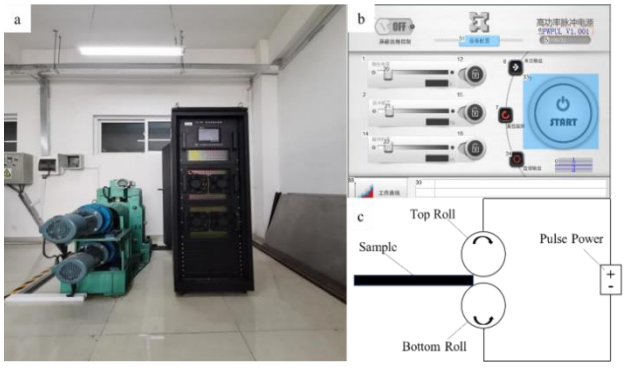

Figure 1 Schematic diagram of high intensity pulse rolling equipment and its working principle: (a) strong pulse rolling equipment, (b) strong pulse power control panel, (c) schematic diagram of electric pulse rolling principle

The specific rolling experimental steps are as follows: (1) use the wire cutting equipment to cut the sample into 60×12×3mm AZ91D magnesium alloy sheet (2) the cut sample will polish off its processing layer with 400# sandpaper and cleaned with ethanol ultrasonic for 5min. (3) the sample to roll will held in 150℃ electric furnace for 10min and then quickly removed for pre-rolling, the amount of pressure down is 1%. (4) the pre-rolled sample will held in 150℃ electric furnace insulation for 10min to remove residual stress, a single pass large amount of depression (20%) electric pulse rolling. The rolling parameters show in Table 2.

Table 2 Rolling parameters

Sample	Voltage (V)	Frequency (Hz)	Pulse width(μs)	Current density(A/mm^2)	Roller temperature(℃)
CR	200	600	20	342	25
EPC-CR	200	600	20	342	27
HR	200	600	20	342	124
EPC-HR	200	600	20	342	119

2.3 Analysis, testing and calculation methods

The samples of AZ91D magnesium alloy after all four rolling processes intercepted from the middle position for testing. The samples polished and electrolytically polished and then analyzed by EBSD using a thermal field emission scanning electron microscope (ZEISS-Sigma 500), where the electrolytic polishing solution was 10% perchloric acid alcohol solution. To further investigate the mechanical properties of AZ91D magnesium alloy after electric pulse rolling, the microhardness test of AZ91D magnesium alloy matrix and Mg17Al12 second phase before and after rolling carried out using HXD-1000TM microhardness tester. The test conducted with an experimental load of 4.9N, a load loading time of 15s, and 10 points for each AZ91D magnesium alloy sample matrix and Mg17Al12 second phase, and the average value of their microhardness taken. CMT5305 type microcomputer-controlled electronic universal testing machine for room temperature tensile performance testing, tensile specimen sample size in line with the GB/T228-2002 calibration selected rectangular equal scale reduction specimens.

The Mg crystal belongs to the dense hexagonal structure, the space point group code is P63/MMC, the lattice constants are A = B =0.3209, C =0.5211, α=β=90°, γ=120°. The Mg crystal model cut, and the Mg base plane thin plate model and prismatic plane thin plate model cut respectively, as shown in Figure 2. Each thin plate model contains 96 atoms, and the thin plate is directly set with a 1.5nm vacuum layer. In this paper, the first-principle method based on density functional theory (DFT) was used for calculation, and the CASTEP module used to optimize and calculate the structure of Mg crystal model. The PBE in generalized Gradient approximation (GGA) used as the exchange correlation functional in calculation. The self-consistent field method (SCF) used to solve the Kohn-Sham equation. Among them, the convergence value of SCF energy is 1.0×10-5 eV/atom. The plane wave cutoff energy is set to 400 eV. The calculated convergence accuracy is 1.0×10-5 eV/atom. The maximum number of self-consistent

iterations is 1000.The maximum convergence accuracy of the force on each atom is 0.01 eV/A. The K Point of the first Brillouin zone was set as 2×4×1. The internal stress convergence standard of the crystal was 0.05 GPa. The external electric field intensity was set as 0.1 eV. The direction was parallel to the Z-axis. The above parameters are used to optimize the geometry of the Mg crystal model. The lattice constants after optimization show in Table 3, and the error between them and the reference value is within 1%, which further proves the accuracy of the calculation in this section.

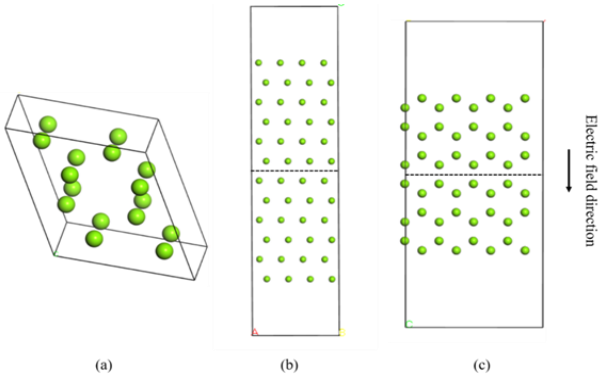

Figure 2 Calculation model: (a) Mg crystal model, (b) Mg basal plane model, (c) Mg prismatic surface model)

Table 3 Lattice parameters of Mg

	Mg	
	a/nm	c/nm
Cal	0.3209	0.5210
Ref[13]	0.3209	0.5211

3 Results and Discussion

3.1 Morphology of rolled pieces

Figure 3 shows the sample morphology of AZ91D magnesium alloy rolled under different rolling conditions. It can see from the surface morphology of AZ91D magnesium alloy after rolling that the surface crack and edge crack of AZ91D magnesium alloy obviously improve under electric pulse rolling. Under the ordinary cold rolling condition, large cracks and small edge cracks appeared on the surface of the sample from the boundary to the middle position. Under the condition of electric pulse cold rolling, only a few edge cracks appear on the surface of AZ91D magnesium alloy samples, which significantly improves compared with that under the condition of ordinary cold rolling. Under ordinary hot rolling condition, fine boundary cracks appear on the surface of AZ91D magnesium alloy samples, and the surface morphology is similar to that under electric pulse cold rolling condition. Under the condition of electric pulse hot rolling, there is no obvious crack on the surface of AZ91D magnesium alloy sample, and the edge crack obviously improves. The results indicate that electric pulse rolling can obviously improve the surface crack of AZ91D magnesium alloy.

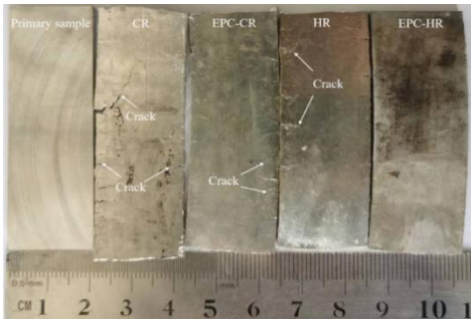

Figure 3 Morphology of AZ91D magnesium alloy samples rolled under different rolling conditions

3.2 Effect of electric pulse rolling on texture of AZ91D magnesium alloy

Figure 4 shows the EBSD image and pole diagram of AZ91D magnesium alloy after rolling with different process parameters. Figure 4a and 4b show the EBSD images of the samples after ordinary cold rolling and electric pulse cold rolling, respectively. It can clearly see from the figure the texture strength of the samples after electric pulse cold rolling in the direction of 0002 and 1010 decreases significantly, from 18.11 and 6.51 to 15.89 and 6.27, respectively. Figure 4c and 4d show the EBSD images of the samples after ordinary hot rolling and electric pulse hot rolling, respectively. After electric pulse applies to the hot rolled samples, the texture strengths in both directions of 0002 and 1010 also decrease, from 9.4 and 3.2 to 5.03 and 1.63.

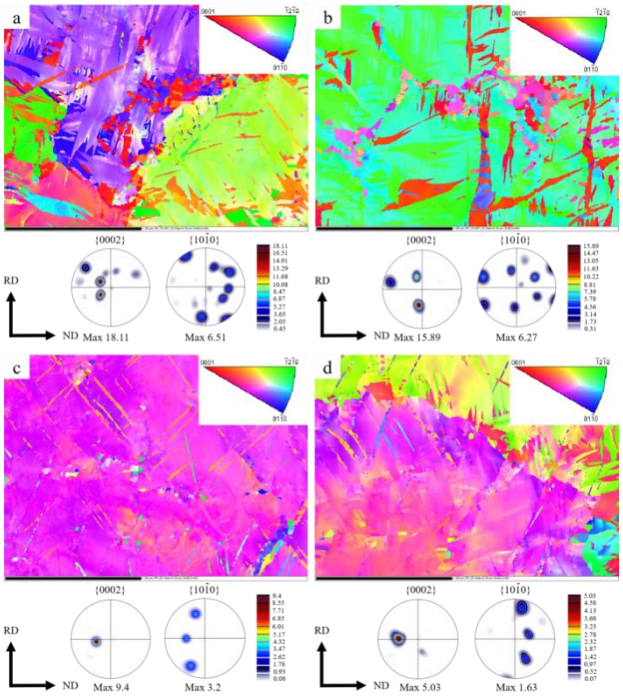

Figure 4 EBSD image of AZ91D magnesium alloy after rolling with different process parameters: (a) ordinary cold rolling, (b) electric pulse cold rolling, (c) ordinary hot rolling, d electric pulse hot rolling)

3.3 Effect of electric pulse rolling on twinning of AZ91D magnesium alloy

Figure 5 shows EBSD images of labeled twin grain boundaries of AZ91D magnesium alloy after rolling with different process parameters. The red line represents {1012} stretched twin boundary, the blue line represents {1011} compressed twin boundary, and the green line represents {1012}-{1011} secondary twin boundary. Figure 5a and 5b show the samples after ordinary cold rolling and electric pulse cold rolling respectively, while Figure 5c and 6d show the samples after ordinary hot rolling and electric pulse hot rolling respectively. EBSD images of labeled twinned grain boundaries of cold-rolled and hot-rolled samples show the content of twinned grain in hot-rolled samples is significantly lower than that in cold-rolled samples. This is because the increase of temperature reduces the Critical Resolved Shear Stress (CRSS) of magnesium alloy non-basal slip system. More slip systems involve in the plastic deformation of magnesium alloy. However, in the cold rolling process at room temperature, only two basal slip systems share in the plastic deformation, which is not enough to completely coordinate the grain deformation, so twin deformation will occur. Therefore, the content of twins in cold rolled samples is significantly higher than that in hot rolled samples. EBSD images of labeled twin grain boundaries of the samples after ordinary rolling and electric pulse rolling show the twin content of the samples with electric pulse rolling is slightly lower than that of the samples without electric pulse rolling at the same temperature. For cold rolled samples, the twin content increases from 8.64% to 15.1% after electric pulse rolling. For the hot rolled sample, the twinning content of the sample increased from 1.66% to 3.24% after electric pulse application. The twin grain boundaries contents of the samples rolled with electric pulse rolling are higher but not lower than those of the samples rolled without electric pulse.

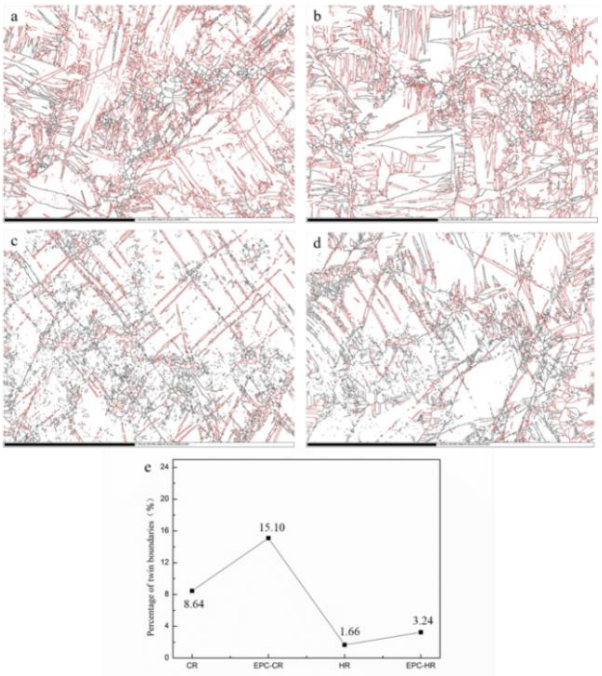

Figure 5 EBSD images of labeled twin grain boundaries of AZ91D magnesium alloy under different rolling parameters:(a) the ordinary cold rolled sample, (b) the electric pulse cold rolled sample, (c) the ordinary hot rolled sample, (d) the electric pulse hot rolled sample

3.4 Effect of electric pulse rolling on orientation difference distribution of AZ91D magnesium alloy

Figure 6 shows the distribution of grain boundary Angle orientation difference of AZ91D magnesium alloy after rolling with different process parameters. Figure 6a and 6b show the distribution of grain boundary Angle orientation difference after ordinary cold rolling and electric pulse cold rolling, respectively. Figure 6c and 6d show the distribution of grain boundary Angle orientation difference after ordinary hot rolling and electric pulse hot rolling, respectively. It can see from the figure that all the rolled samples under the four different processes have a peak at ~86°, and the peak of ~86° in the sample after electric pulse application is significantly higher than that in the sample without electric pulse application, showing the introduction of pulse current promotes the generation of tensile twins in AZ91D magnesium alloy, which is consistent with EBSD image analysis of twin grain boundaries. The peak of ~40° appeared in the hot rolled sample, which obviously reduced after the application of electric pulse. In addition, the small Angle grain boundary content of < 5° decreased after the application of electric pulse. For the cold rolled sample, the small Angle grain boundary content of < 5° decreased from 71% to 63% after the application of pulse current. For the hot rolled sample, the grain boundary content of small Angle < 5° decreased from 79% to 77% after pulse current application.

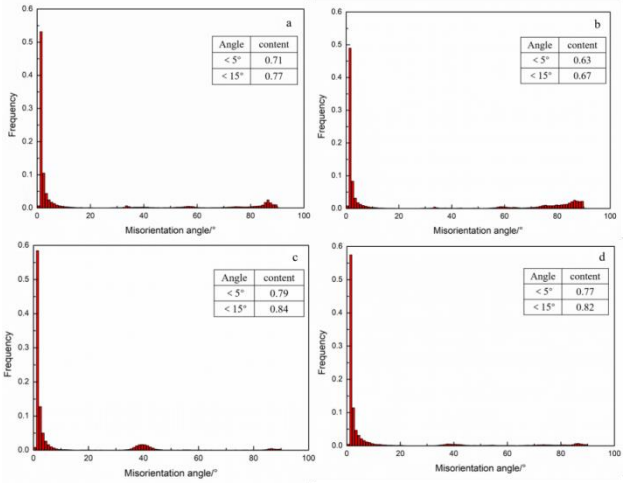

Figure 6 Distribution of grain boundary angular orientation difference of AZ91D magnesium alloy after rolling with different process parameters:(a) the ordinary cold rolled sample, (b) the electric pulse cold rolled sample, (c) the ordinary hot rolled sample, (d) the electric pulse hot rolled sample

3.5 Effect of electric pulse rolling on microhardness of AZ91D magnesium alloy

Figure 7 shows the microhardness of each phase of AZ91D magnesium alloy after rolling with different process parameters. As can be seen from the figure, the microhardness of α-Mg matrix of the cold-rolled sample decreases by 15.7% from 61.1HV to 51.5HV after pulse

current application, which is 8.1% lower than that of the original unrolled AZ91D magnesium alloy sample of 56.1HV. The microhardness of α-Mg matrix decreased from 60.5HV to 51.5HV by 14.8%, which was 8.1% lower than that of original unrolled AZ91D magnesium alloy sample (56.1HV).

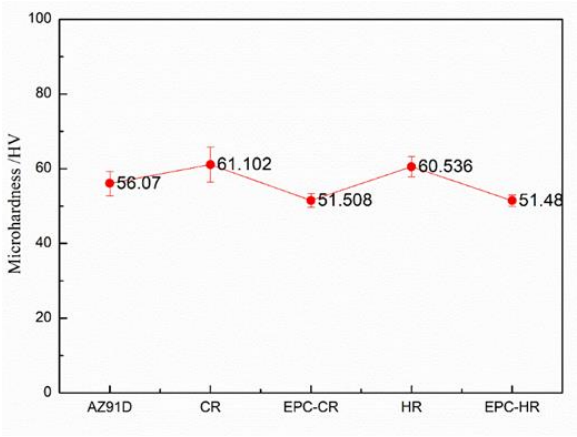

Figure 7 Microhardness of AZ91D magnesium alloy phases after rolling with different process parameters

3.6 Effect of electric pulse rolling on tensile properties of AZ91D magnesium alloy

Figure 8 shows the average tensile strength and average elongation of AZ91D magnesium alloy after rolling with different process parameters. As can see from the figure, the tensile strength of the rolled AZ91D magnesium alloy sample is significantly higher than that of the unrolled original AZ91D magnesium alloy sample. The elongation of the ordinary cold rolled AZ91D magnesium alloy sample is lo``wer than that of the unrolled original AZ91D magnesium alloy sample. For the cold-rolled samples, the tensile strength and elongation increased from 106MPa and 1.5% to 127MPa and 3.5%, respectively. For the hot rolled samples, the tensile strength and elongation increased from 137MPa and 3.4% to 169MPa and 4.7%.

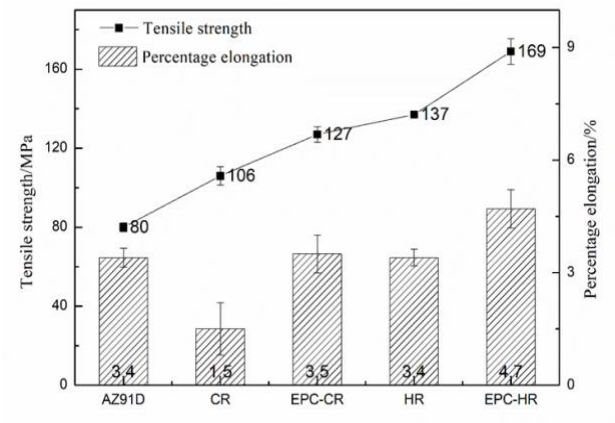

Figure 8 Tensile properties of AZ91D magnesium alloy after rolling with different process parameters

Figure 9 shows SEM images of fracture of AZ91D magnesium alloy rolled with different process parameters. Figure 8a shows the fracture morphology of unrolled original AZ91D magnesium alloy sample. Figure 8b and 8c show the fracture morphology of AZ91D magnesium alloy after ordinary cold rolling and electric pulse cold rolling respectively. Figure 8d and 8e show the fracture morphology of AZ91D magnesium alloy after ordinary hot rolling and electric pulse hot rolling respectively. It can see from the figure that, There are a lot of cracks and dissociation steps in the fracture of unrolled AZ91D magnesium alloy samples, and there is no dimple, so AZ91D magnesium alloy mainly presents brittle fracture. The fracture morphology of AZ91D magnesium alloy after common cold rolling is similar to that of original AZ91D magnesium alloy, both of which have many cracks and dissociation steps. The fracture of AZ91D magnesium alloy after electric pulse cold rolling has a dimple also cracks and dissociation steps. Similar to cold rolling, there are many cracks and dissociation steps in the fracture of AZ91D magnesium alloy after ordinary hot rolling, and there are almost no dimples. However, there are cracks and dissociation steps in the fracture of AZ91D magnesium alloy after electric pulse hot rolling, with many dimples, and the fracture types are mainly brittle fracture and ductile fracture.

Figure 10 shows the fixed-point EDS images of the fracture of AZ91D magnesium alloy rolled with different process parameters. EDS spectra analyzed at the crack and dissociation step at point 1 and point 2, respectively, and at the dimple at point 3. According to the results of energy spectrum analysis, the crack and dissociation step are the mixed phase of β-Mg17Al12 phase and α-Mg phase, while the dimple is α-Mg matrix phase. It can see the α-Mg matrix changes from the brittle phase to the ductile phase after pulse current application, which improves the elongation of AZ91D magnesium alloy.

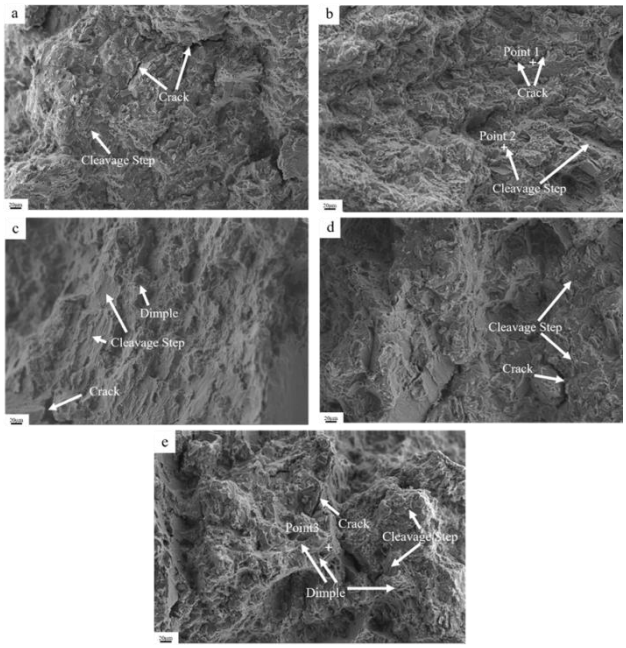

Figure 9 SEM images of fracture of AZ91D magnesium alloy rolled with different process parameters: (a) the original unrolled sample, (b) the ordinary cold rolled sample, (c) the electric pulse cold rolled sample,(d) the ordinary hot rolled sample, (e) the electric pulse hot

rolled sample

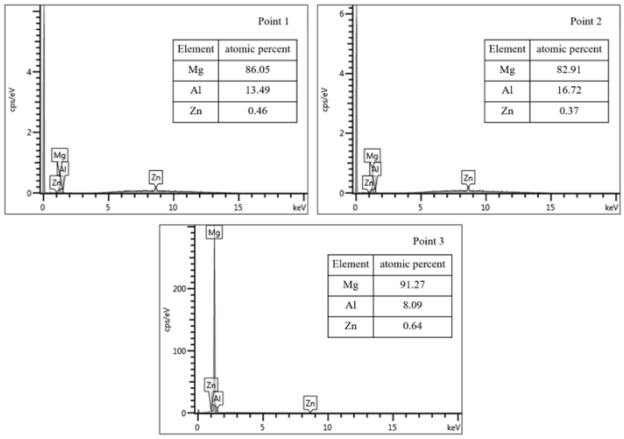

Figure 10 Image of EDS energy spectrum analysis

3.7 First principles computational analysis

3.7.1 Mechanical properties

The effect of electric field on mechanical properties of Mg studied by first principles calculation method. The elastic constant Cij of Mg before and after electric field application calculated, and the anisotropy characteristics of Mg under applied electric field further studied. The bulk modulus B, shear modulus G, Young's modulus E and Poisson's ratio V were mainly calculated. The calculation results show in Table 4. The bulk modulus B refers to the ability of a material to resist compression deformation under applied external stress. For solid materials, within their elastic limits, the larger the volume modulus B is, the stronger the compression deformation resistance is. As can see from Table 4, after the electric field applies, the volume modulus B of Mg increases, and it becomes difficult to compress. Shear modulus G refers to the ability of a material to resist shear strain under shear stress. When the value of shear modulus G of a material increases, its stiffness increases. It can see from Table 4 that after the application of electric field, Mg's shear modulus G decreases, and its stiffness becomes weaker. Young's modulus E is within the elastic limit, the material is the ratio of stress and the stress caused by the strain, with the same shear modulus, the higher the value of young's modulus E, the stronger the stiffness of the material. From the table 4 shows that after applying an electric field, the value of young's modulus E of Mg decreased, its stiffness weak, are consistent with the shear modulus. Poisson's ratio v refers to when the material to be pull (pressure) stress, transverse and axial strain ratio, the greater the material poisson's ratio value, its plasticity, the better [14]. From table 4 shows that after applying an electric field, poisson's ratio of Mg values increase, its plasticity is also improved, with the former analysis of the tensile fracture surface consistent. The elastic modulus ratio B/G can be used to evaluate the brittleness and plasticity of the material. When the value of B/G is greater than 1.75, the material exhibits ductility, and the larger the value, the better the plasticity of the material, and otherwise, the material exhibits brittleness. As can see from Table 4, the B/G value of Mg increased significantly by 1.75 after the electric field applied. Its plasticity improve. Hardness H is an important index for evaluating material properties, which refers to the ability of the material to resist hard objects pressing into the surface locally. It can see from Table 4 the hardness of Mg decreases significantly after the electric field applies, which is consistent with the experimental results above and further proves the accuracy of the calculation.

Table 4 Calculation results of mechanical properties of Mg before and after electric field application

	B/GPa	G/GPa	E/GPa	v	A	B/G	H/GPa
Mg	36.38	16.41	42.78	0.3	0.3	2.21	2.14
EP-Mg	52.60	14.47	39.77	0.37	0.45	3.64	1.21

3.7.2 Generalized layered fault energy

The generalized layered fault energy refers to the energy difference between the crystal cells per unit area on a certain slip surface before and after the formation of layered fault. The formula for calculating the generalized layered fault energy γ is:

$$\gamma = \frac{E-E_0}{A} \quad (3\text{-}1)$$

Where, E0 is the total energy of the intact crystal, E is the total energy of the crystal after lamination, and A is the lamination area.

The total energy of the complete crystal structure of Mg system obtained by structural relaxation of the thin plate model of Mg base plane and prismatic plane. The total energy of the layered fault structure calculated by structural relaxation of 0.1b for each slip plane movement. The calculated data were put into Equation 3-1 to obtain the generalized layered fault energy. It generally believes the size of the unstable fault energy γus indicates the difficulty of the slip system along the slip plane. The larger the value of γus, the more difficult the slip is to start, and the worse the plastic forming ability of the material is. The generalized layered fault energy of Mg's base plane and its prismatic plane before and after applying electric field calculates by the above method, and the calculation results are shown in figure 11.

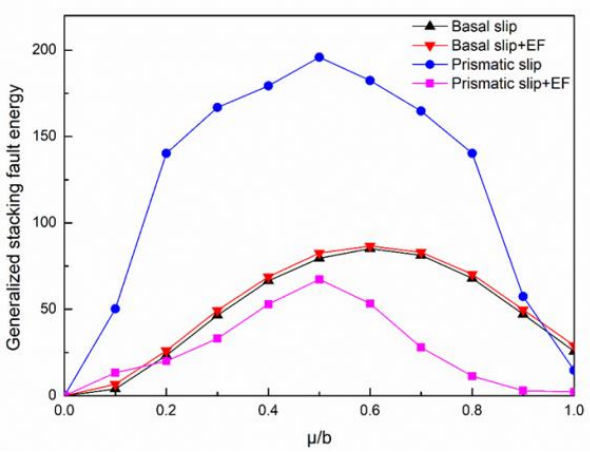

Figure 11 Generalized layered fault energy curves of

Mg base plane and prism plane before and after electric field application

As can see from figure 10, when no electric field applies, the generalized layered fault energy of Mg prism surface is significantly larger than that of its base surface. The unstable layered fault energy of Mg prism surface is γus=196mJ/m^2. The unstable layered fault energy of Mg base surface is γus=80mJ/m^2, showing that under ordinary conditions, Mg prism slip system is more difficult to start than the base slip system. This is also confirmed by the deformation theory of Mg. After the electric field is applied, the generalized layered fault energy of Mg base surface does not change much, and its unstable layered fault energy γus remains about 80mJ/m^2. However, after the electric field applies, the generalized layered fault energy of Mg prism surface decreases significantly, and its unstable layered fault energy γus decreases from 196mJ/m^2 to 67mJ/m^2. The results show the Mg prismatic slip system is easier to start after the electric field is applied, and thus the plastic forming ability of Mg is improved.

Poty et al. [15] studied the dislocation mobility of Zr and Ti with dense hexagonal structure by measuring the ratio of γuS (basal) layer fault energy to Prism (Prism) layer fault energy. It is reasonable to use the ratio of basal and Prism unstable layer fault energy γus as the criterion of Mg anisotropy. For table 5 Mg base level before and after applying an electric field and layer on the surface of the prism is not stable can gamma us wrong and its ratio. From the data in table 5 shows that after applying an electric field model of Mg base unstable layer can wrong with prismatic surface instability fault energy ratio closer to 1. The above experimental results show the introduction of the electric field can reduce the strength of the base surface texture, therefore. The introduction of electric field improves the anisotropy of Mg, which leads to the reduction of basal texture, and then makes Mg have higher formability.

Table 5 Unstable layered fault energies γus and their ratios at Mg base and prismatic surfaces before and after electric field application

	γ_{us}(basal)	γ_{us}(prism)	γ_{us}(basal)/γ_{us}(prism)
Mg	85.12	182.41	0.46
EP-Mg	86.66	67.36	1.28

4 Conclusion

(1) Pulse current applied in the rolling process of AZ91D magnesium alloy can effectively improve the edge crack of the sample, optimize the texture of AZ91D magnesium alloy and reduce its texture strength. In addition, pulse current can promote the formation of tensile twins and the transition from small Angle grain boundaries to large Angle grain boundaries, which improves the plastic forming ability of AZ91D magnesium alloy.

(2) When pulse current is applied during AZ91D magnesium alloy rolling, the microhardness of α-Mg matrix decreases by about 15% compared with ordinary rolling. The tensile strength and elongation increased from 137MPa and 3.4% to 169MPa and 4.7%, respectively. In addition, dimples appear in the AZ91D magnesium alloy samples after electric pulse rolling, and dimples are concentrated in the α-Mg matrix, showing the introduction of pulse current can promote the transition from brittle to ductile fracture of AZ91D magnesium alloy.

(3) After the application of electric field, the stiffness of Mg decreases, the Poisson's ratio of Mg increases, and the B/G value increases significantly by 1.75, which improves its plasticity.

(4) When the electric field is applied, the fault energy of Mg's base surface does not change much. But the fault energy of Mg's prismatic surface decreases obviously, showing the external electric field mainly affects Mg's prismatic surface slip, which makes Mg's prismatic surface slip easier to start, and thus improves the plastic forming ability of Mg.

Acknowledgments

The work was supported by the National Natural Science Foundation of China [grant number 52061002].

Conflict of Interest Statement

All authors disclosed no relevant relationships.

References

[1] X. Hao, W.X. Hao, G.H. Geng, et al.. Effects of High-Density Pulse Currents on the Solidification Structures of Cu-SiCp/AZ91D Composites Advances in Materials Science and Engineering. 2019(1): 1-6.

[2] Y. Xu, C. Chen, X.X. Zhang, et al.. Dynamic recrystallization kinetics and microstructure evolution of an AZ91D magnesium alloy during hot compression Materials Characterization. 2018(145): 39-52.

[3] W.J. Li, K.K. Deng, X. Zhang, et al.. Microstructures, tensile properties and work hardening behavior of SiCp/Mg-Zn-Ca composites Journal of Alloys and Compounds. 2017(695): 2215-2223.

[4] K. Edalati, R. Uehiro, Y. Ikeda, et al.. Design and synthesis of a magnesium alloy for room temperature hydrogen storage Acta Materialia. 2018(149): 88.

[5] J. Kuang, X.H. Li, R.K. Zhang, et al.. Enhanced rollability of Mg-3Al-1Zn alloy by pulsed electric current: a comparative study Materials & Design. 2016(100): 204.

[6] J. Kuang, X.H. Li, R.K. Zhang, et al.. Enhanced rollability of Mg-3Al-1Zn alloy by pulsed electric current: a comparative study Materials & Design. 2016(100): 204.

[7] P.J. Zhao, Z.H. Chen, C.F. Dong. Damage and Failure Analysis of AZ31 Alloy Sheet in Warm Stamping Processes Journal of Materials Engineering and Performance. 2016,25(7):2702.

[8] N. Stanford, R.K.W. Marceau, M.R. Barnett. The effect of high yttrium solute concentration on the twinning behaviour of magnesium alloys Acta Materialia. 2015(82):447.

[9] I. Indhiarto, T. Shimizu, M. Yang. Effect of Peak Current

Density on Tensile Properties of AZ31B Magnesium Alloy Materials. 2021, 14(6):5.

[10] K. Liu, X.H. Dong, H.Y. Xie, et al.. Influence of pulsed current on deformation mechanism of AZ31B sheets during tension Journal of Alloys and Compounds. 2016(676): 106.

[11] Vitek, V. Intrinsic stacking faults in body-centred cubic crystals. Philosophical Magazine,1968, 18(154): 773-786.

[12] M. Yuasa, M. Hayashi, M. Mabuch, et al.. Improved plastic anisotropy of Mg-Zn-Ca alloys exhibiting high-stretch formability: A first-principles study Acta Materialia. 2014(65): 207.

[13] Guangyin Yuan, Yangshan Sun, Wenjiang Ding. Effects of Sb addition on the microstructure and mechanical properties of az91 magnesium alloy. Scripta Materialia, 2000, 43(11): 1009-1013.

[14] S. Sandlobes, M. Friak, S. Zaefferer, et al.. The relation between ductility and stacking fault energies in Mg and Mg-Y alloys Acta Materialia. 2012, 60(6-7): 3011.

[15] Zhang J, Mao C, Long C G, et al.. Phase stability, elastic properties and electronic structures of Mg-Y intermetallics from first-principles calculations[J]. Journal of Magnesium & Alloys, 2015, 3(2): 127-133.

[16] S.F. Matar, R. Pottgen, B. Chevalier. Electronic and magnetic structures and bonding properties of Ce_2T_2X (=nd element; X = Mg, Cd, Pb or Sn) intermetallics from first principles Intermetallics. 2014(51): 18.